



OPEN Strain-specific differences in cerulein-induced acute and recurrent acute murine pancreatitis

Alexandra Demcsák¹, Thanh Tran², Miklós Sahin-Tóth¹ & Andrea Geisz-Fremy²✉

Hyperstimulation with the secretagogue cerulein is a commonly used experimental model to study acute, recurrent acute and chronic pancreatitis in mice. Earlier studies showed that inbred mouse strains had different susceptibility to cerulein-induced pancreatitis. Here, we confirm and extend these findings by characterizing the severity of acute and recurrent acute pancreatitis in the C57BL/6N and FVB/N strains. When acute pancreatitis was induced with repeated cerulein injections, FVB/N mice had more severe pancreatic edema, higher plasma amylase levels, increased inflammatory cell infiltration, and more extensive acinar cell necrosis relative to the C57BL/6N strain. Cerulein elicited higher and more sustained trypsin activity in FVB/N mice relative to C57BL/6N animals, which was likely due to the lower expression of the SPINK1 trypsin inhibitor and the trypsinogen-degrading lysosomal protease cathepsin L. In C57BL/6N mice, we previously showed that pancreatitis responses were more severe during a second attack compared with the initial, sentinel episode. In FVB/N mice, we now found that the second episode was associated with lower pancreas edema and plasma amylase but higher inflammatory cell infiltration than the first attack. The observations reinforce the notion that inbred mouse strains exhibit differences in their pathological responses during acute and recurrent acute pancreatitis.

Keywords Acute pancreatitis, Recurrent acute pancreatitis, Cerulein-induced pancreatitis, Mouse models, C57BL/6N, FVB/N

Pancreatitis is the inflammatory disorder of the pancreas which clinically can present as acute, recurrent acute, and chronic pancreatitis¹. These diseases often form a continuum where the initial, so-called sentinel episode of acute pancreatitis progresses to recurrent attacks and eventually chronic pancreatitis^{1–3}. Progression is typically driven by environmental and/or genetic risk factors^{4,5}. To understand the mechanistic basis of the disease, scientist routinely employ mouse models in which pancreatitis is induced through various forms of artificial injury. Some models are designed to mimic clinical etiologies, such as high-fat diet, alcohol consumption, or ductal obstruction^{6–8}. While exceedingly rare, human pancreatitis can also result from exposure to potent cholinergic agonists, such as scorpion venom or certain insecticides^{9,10}. This phenomenon can be replicated experimentally by administering supraphysiologic concentrations of the secretagogue hormone cholecystokinin (CCK) or its analog, cerulein. The secretagogue hyperstimulation method is one of the most widely used experimental pancreatitis models¹¹. This approach is noninvasive, highly reproducible, and, by varying the dose and duration of administration, it allows investigators to study features of acute, recurrent acute and chronic pancreatitis, as well as pancreatic regeneration.

Using the C57BL/6N inbred mouse strain, we recently demonstrated that repeated episodes of cerulein-induced pancreatitis exhibited increased severity relative to the sentinel episode¹². Furthermore, we found that cerulein-induced intrapancreatic trypsin activity does not mediate the pathological responses in this strain¹³. Whether or not these observations would hold true for other laboratory strains of mice remains to be determined. In this regard, several prior studies indicated that the genetic background of mice can influence disease outcomes in experimental pancreatitis protocols^{14–20}.

In the current study, we set out to compare acute pancreatitis responses in two inbred strains, the C57BL/6N and FVB/N mice. In recent years, several genetically altered mouse models of pancreatitis were created and characterized in the C57BL/6N background, such as various trypsinogen mutant and chymotrypsin-deficient mice^{21–29}. It has remained unclear, however, to what degree the particular genetic background of C57BL/6N mice might have contributed to the reported pancreatitis phenotypes of these strains. For comparison, we chose FVB/N mice because earlier studies reported increased severity relative to the C57BL/6 J strain, a different

¹Department of Surgery, University of California Los Angeles, Los Angeles, CA 90095, USA. ²Department of Surgery, Boston University, 700 Albany Street, W408G, Boston, MA 02118, USA. ✉email: geisz@bu.edu

substrain of C57BL/6 mice^{17,19}. In our experiments, we compared the severity of cerulein-induced acute pancreatitis and the extent of cerulein-induced intrapancreatic protease activation in the two experimental mouse strains. Furthermore, we induced recurrent acute pancreatitis in FVB/N mice and compared disease responses during the sentinel and second episodes.

Results

Cerulein-induced acute pancreatitis in C57BL/6N and FVB/N mice

To compare acute pancreatitis severity, we challenged FVB/N and C57BL/6N mice with 10 hourly injections of cerulein and euthanized them 1 h after the last injection (Fig. 1A). Pancreas edema was assessed by measuring the pancreas weight (Fig. 1B) and the pancreatic water content (Fig. 1C). In both strains, cerulein treatment induced a significant increase in these parameters relative to control mice given saline. These changes were significantly more pronounced in FVB/N mice than C57BL/6N animals. Similarly, repeated cerulein injections induced a significant increase in plasma amylase activity relative to saline-treated mice, which was significantly

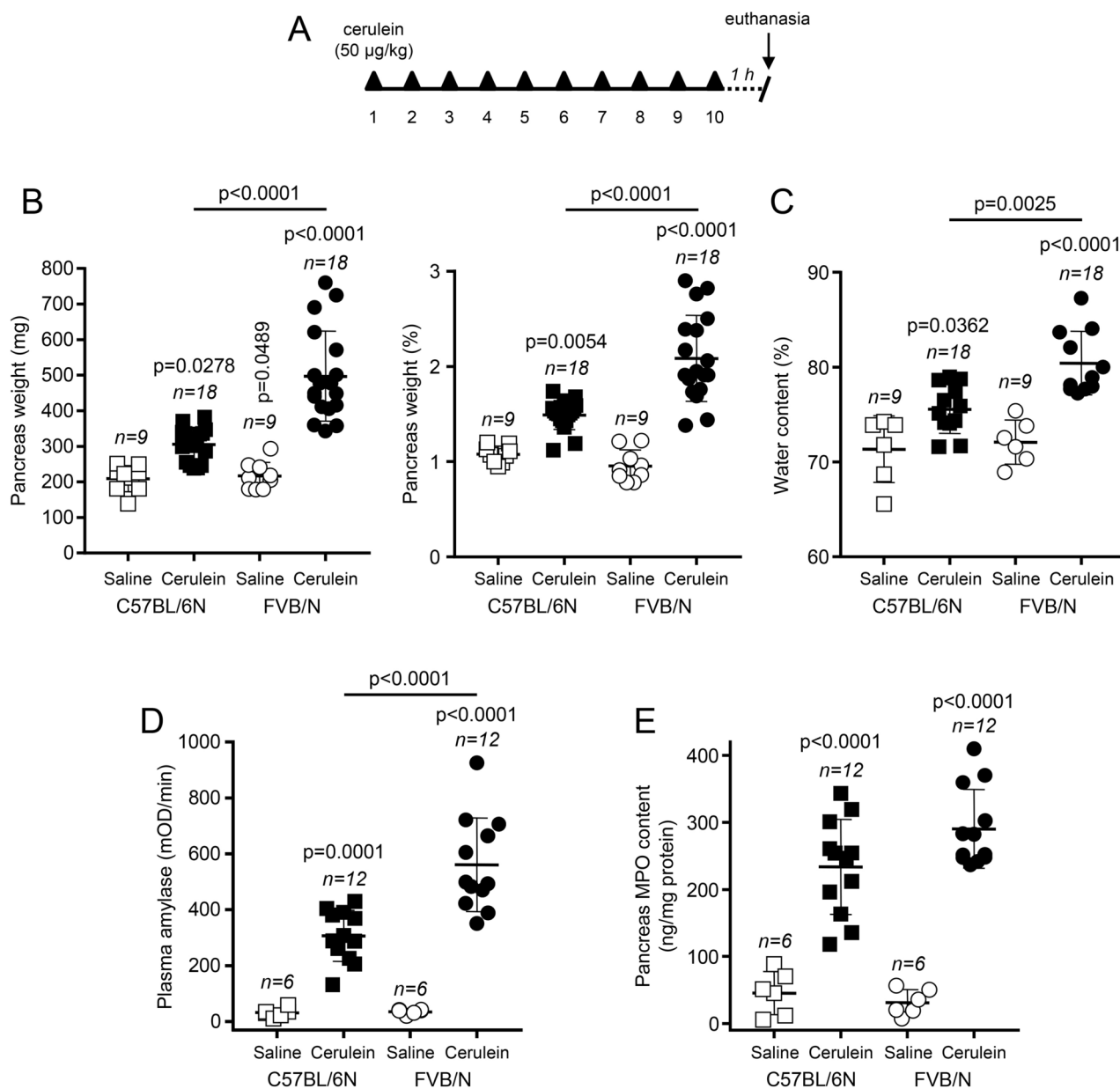


Fig. 1. Cerulein-induced acute pancreatitis in C57BL/6N and FVB/N mice. **(A)** Experimental protocol. Solid triangles indicate injections of saline or cerulein. Mice were euthanized 1 h after the last injection. **(B)** Pancreas weight in mg units and expressed as percent of body weight. **(C)** Pancreatic water content. **(D)** Plasma amylase levels. **(E)** Pancreatic myeloperoxidase (MPO) content. Individual data points with the mean and standard deviation are shown. The difference of means between groups was analyzed by one-way ANOVA and Tukey's post-hoc test.

higher in the FVB/N strain compared with C57BL/6N mice (Fig. 1D). To evaluate neutrophil granulocyte infiltration, we measured pancreatic myeloperoxidase (MPO) levels. Relative to mice given saline, we observed significantly increased MPO activity in response to cerulein treatment in both strains, and a non-significant trend for higher MPO levels in FVB/N versus C57BL/6N mice (Fig. 1E). Histological evaluation (Fig. 2A) and scoring of hematoxylin–eosin-stained pancreas sections from cerulein-treated mice confirmed the significantly higher edema (Fig. 2B) and inflammatory cell infiltration (Fig. 2C) in FVB/N mice relative to C57BL/6N animals. Furthermore, significantly larger areas of acinar cell necrosis were apparent in FVB/N mice when compared to the C57BL/6N strain (Fig. 2D).

Intrapancreatic trypsin and chymotrypsin activities in C57BL/6N and FVB/N mice

To test whether the more severe acute pancreatitis responses observed in FVB/N mice can be attributed to stronger intrapancreatic protease activation, we compared cerulein-induced trypsin and chymotrypsin activities in the two strains. In this experiment, mice received a single saline or cerulein injection and were euthanized 30 min, 2 h, 4 h, and 8 h later (Fig. 3A). We found that cerulein induced significantly increased trypsin (Fig. 3B) and chymotrypsin (Fig. 3C) activities in both strains as early as 30 min after administration. Protease activities then gradually declined over the 8-h time course. The activity peaks were higher in FVB/N versus C57BL/6N mice, but only the difference in trypsin activity reached statistical significance. Interestingly, the rate of decline in protease activity was measurably slower in the FVB/N strain resulting in more sustained intrapancreatic trypsin and chymotrypsin activities.

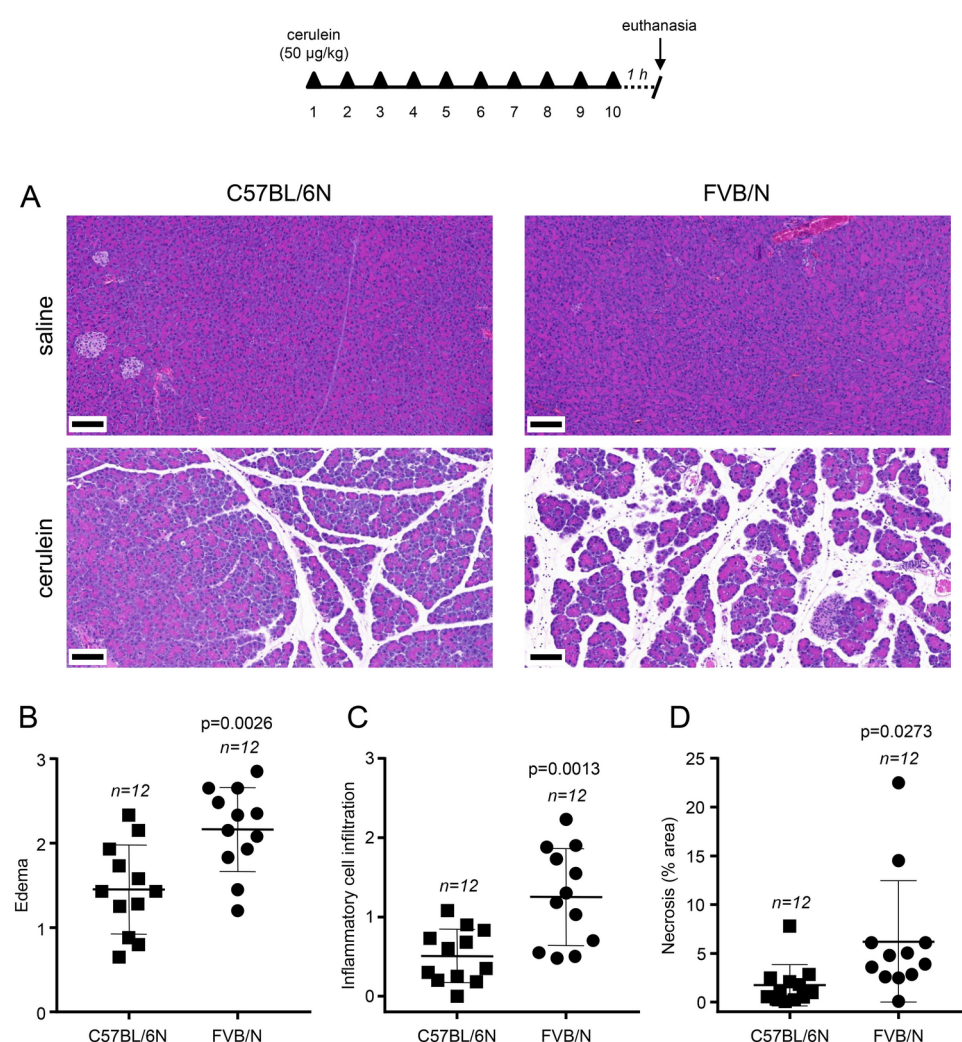


Fig. 2. Histology of cerulein-induced acute pancreatitis in C57BL/6N and FVB/N mice. (A) Representative hematoxylin–eosin-stained pancreas sections are shown from saline and cerulein-treated C57BL/6N and FVB/N mice. Scale bars correspond to 100 μ m. Histological scoring for (B) edema, (C) inflammatory cell infiltration, and (D) necrosis. Individual data points with the mean and standard deviation are shown. The difference of means between groups was analyzed by unpaired *t*-test.

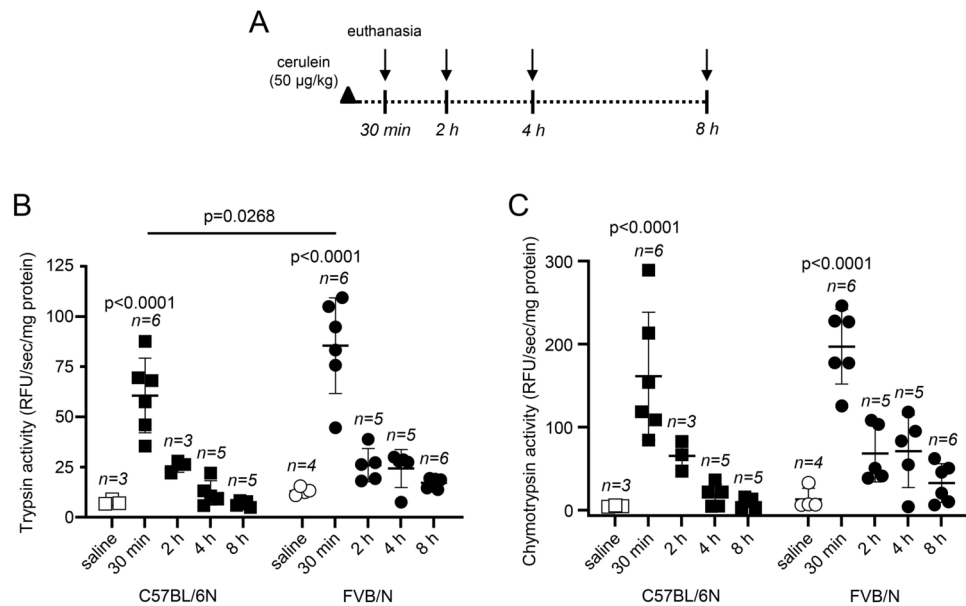


Fig. 3. Cerulein-induced protease activation in the pancreas of C57BL/6N and FVB/N mice. **(A)** Experimental protocol. Solid triangle indicates a single cerulein or saline injection. Arrows indicate the different time points of euthanasia. **(B)** Cerulein-induced intrapancreatic trypsin activity. **(C)** Cerulein-induced intrapancreatic chymotrypsin activity. Individual values with the mean and standard deviation are shown. The difference of means between groups was analyzed by one-way ANOVA and Tukey's post-hoc test.

Protease zymogen, trypsin inhibitor, and lysosomal cathepsin levels in the pancreas of C57BL/6N and FVB/N mice

To investigate the reason behind the different intrapancreatic protease activation kinetics induced by cerulein in the two strains, we used activity assays to measure trypsinogen (Fig. 4A), chymotrypsinogen (Fig. 4B), proelastase (Fig. 4C) and amylase (Fig. 4D) levels, and employed western blotting to assess expression of the mouse cationic (T7) trypsinogen (Fig. 4E), the endogenous trypsin inhibitor serine protease inhibitor Kazal-type 1 (SPINK1) (Fig. 4F) and the lysosomal hydrolases cathepsin B and L (CTSB and CTSL) (Fig. 5A). We also determined the total protein (Fig. 5B) and DNA (Fig. 5C) content of the pancreata. Unexpectedly, we found that protease zymogens, amylase, and SPINK1 levels were lower in the pancreas of FVB/N mice than C57BL/6N animals even though their total protein and DNA contents were comparable. The difference was statistically significant for trypsinogen (~40% less), proelastase (~35% less) and amylase (~20% less). Western blot analysis of pancreas homogenates showed significantly lower expression of cationic (T7) trypsinogen (~20% less) and SPINK1 (~60% less) in FVB/N mice relative to the C57BL/6N strain. The observations indicate that the trypsinogen-to-inhibitor ratio is larger in FVB/N versus C57BL/6N mice, which might explain the higher propensity for intrapancreatic trypsin activation in this strain despite its lower total trypsinogen content. Interestingly, while no difference was observed in the levels of the trypsinogen activator CTSB, we found significantly lower expression of the trypsinogen-degrading enzyme CTSL in FVB/N mice compared to the C57BL/6N strain. Thus, in addition to the reduced SPINK1 expression, low CTSL levels are also presumed to contribute to the increased trypsin activity observed in FVB/N mice.

Sex-specific differences in C57BL/6N and FVB/N mice

We performed subgroup analysis on C57BL/6N and FVB/N mice to evaluate whether biological sex affects pancreatic protein content, intrapancreatic protease activation, and susceptibility to experimental pancreatitis. We found no differences in pancreatic protein content and protease activities between males and females. Although some acute pancreatitis parameters displayed minor variations, there was no significant sex-dependent effect on pancreatitis severity (not shown).

Recurrent acute pancreatitis in FVB/N mice

In a previous study, we used cerulein to induce recurrent acute attacks of pancreatitis in the C57BL/6N strain and found that mice developed more severe acute pancreatitis during the second and third attacks relative to the initial episode¹². We also observed that despite the histological recovery after the initial episode of pancreatitis, there remained an increased number of tissue-resident macrophages that might contribute to the increased severity of recurrent episodes. Here, we employed a similar experimental protocol in FVB/N mice and induced two acute pancreatitis attacks with 10 hourly cerulein injections given 7 days apart. Mice were euthanized 1 h after the last cerulein administration on day 1 (1-episode group), after the 7-day recovery period on day 8 (recovery group), or 1 h after the last cerulein injection on day 8 (2-episode group) (Fig. 6A). During the first episode of acute pancreatitis, significant elevations in pancreas weight (Fig. 6B), pancreatic water content

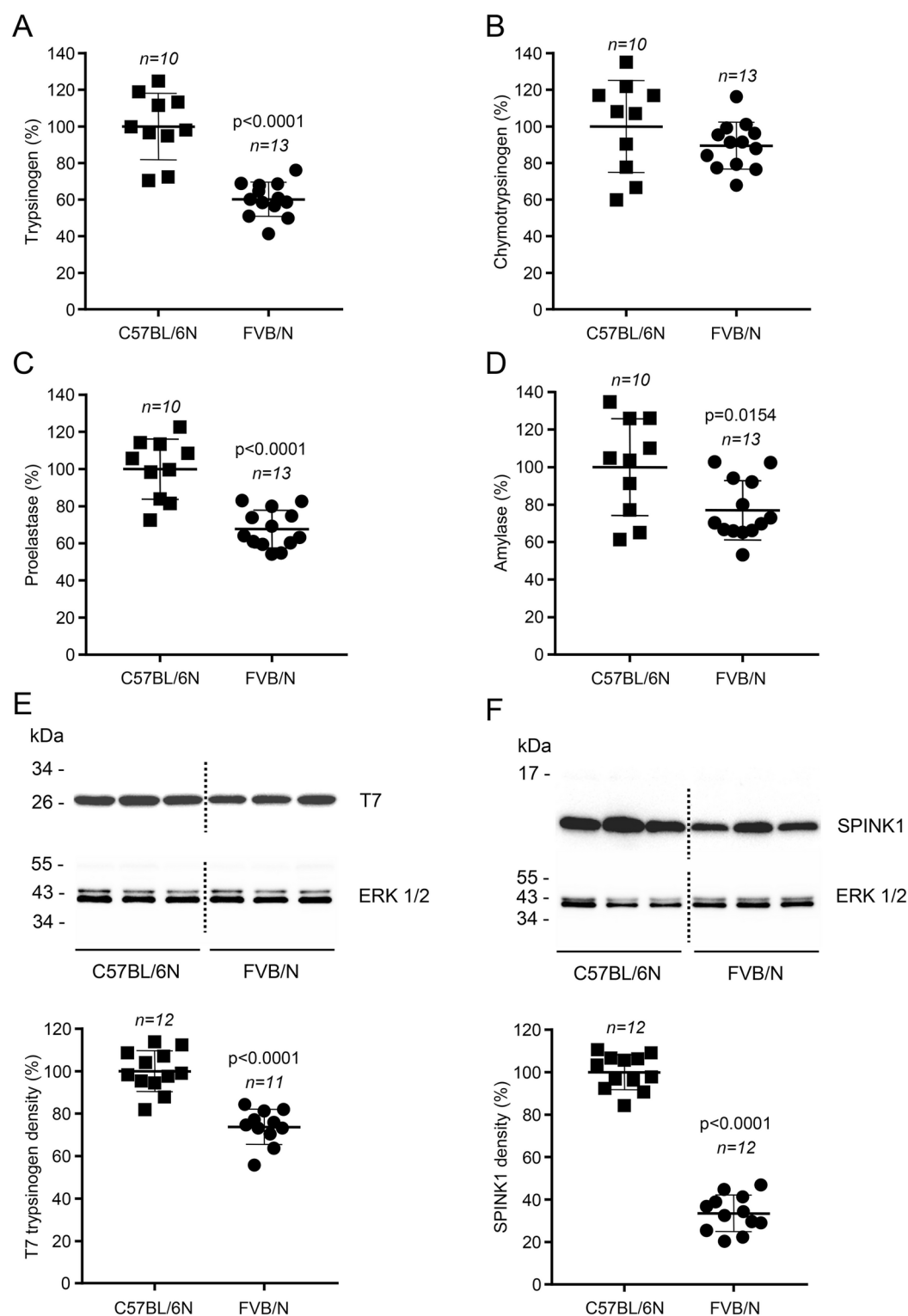


Fig. 4. Protease zymogen and SPINK1 trypsin inhibitor levels in the pancreas of C57BL/6N and FVB/N mice. The total (A) trypsinogen, (B) chymotrypsinogen, (C) proelastase, and (D) amylase content of pancreas homogenates were determined by activity assays, as described in *Methods*. Results were expressed as percent of the average C57BL/6N values. Expression levels of (E) cationic (T7) trypsinogen and (F) SPINK1 protein were assessed by western blotting and densitometry. ERK1/2 was detected as loading control. Representative blots from three experiments are shown. Densitometry results are graphed as individual data points with the mean and standard deviation indicated. The difference of means between groups was analyzed by the unpaired *t*-test.

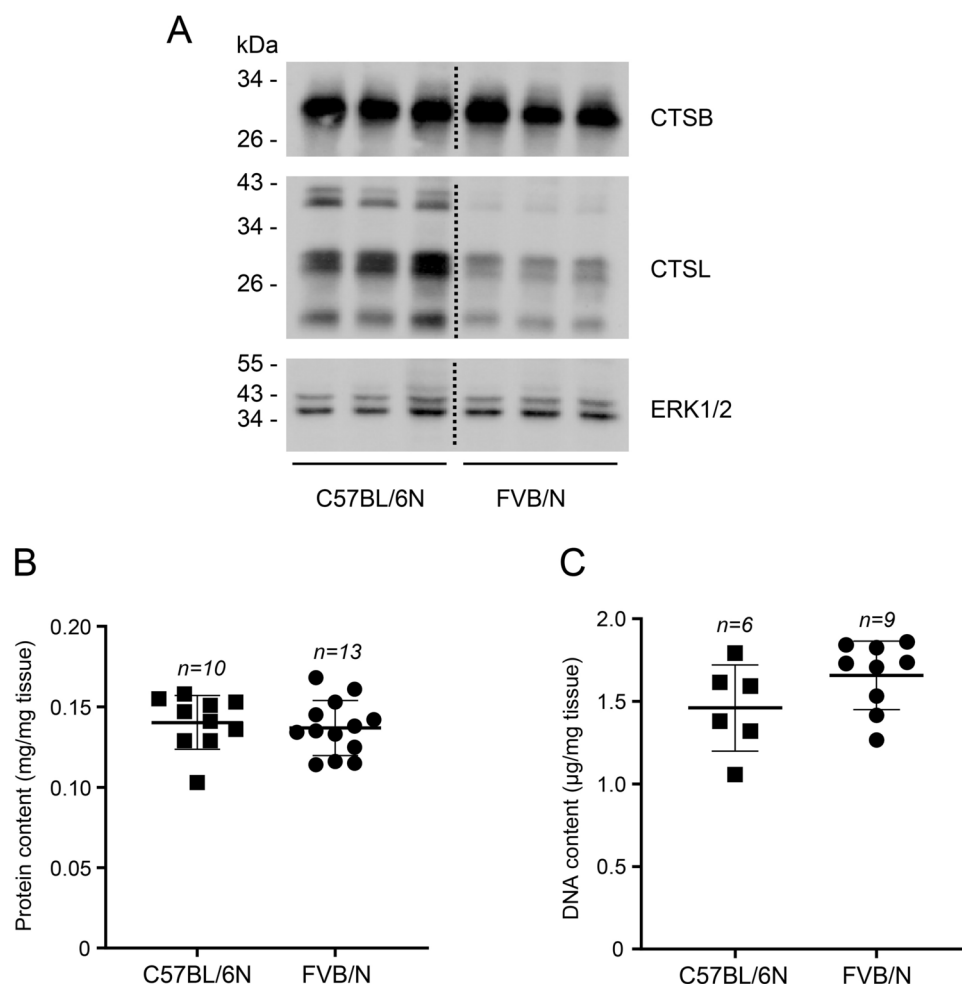


Fig. 5. Lysosomal protease expression, protein content, and DNA content in the pancreas of C57BL/6N and FVB/N mice. **(A)** Western blot analysis of pancreas homogenates to measure cathepsin B (CTSB) and cathepsin L (CTSL) levels was performed as described in *Methods*. ERK1/2 was detected as loading control. **(B)** Total protein and **(C)** DNA content of pancreas homogenates were measured as described in *Methods*.

(Fig. 6C), plasma amylase (Fig. 6D), and pancreatic MPO content (Fig. 6E) were observed, which returned to normal levels following the 7-day recovery period. During the second episode of acute pancreatitis, FVB/N mice exhibited somewhat different pathological responses than reported previously for C57BL/6N mice. Thus, pancreas weight, water content, and plasma amylase were reduced whereas pancreatic MPO content was significantly increased relative to the first episode. When hematoxylin–eosin-stained pancreas sections were evaluated (Fig. 7A), we observed more extensive edema and inflammatory cell infiltration after the second versus the first episode of pancreatitis. Histology scoring of multiple sections confirmed these differences in edema (Fig. 7B) and inflammatory cells (Fig. 7C). We also noted that histological edema and inflammatory cell numbers did not completely normalize by the end of the recovery period after the first episode. Finally, histology scoring indicated that acinar cell necrosis was significantly increased during the first pancreatitis attack, returned to normal by the end of the recovery phase, and remained low during the second episode (Fig. 7D).

Discussion

Several previous studies demonstrated that various inbred mouse strains exhibited different pathological responses in experimental pancreatitis models. Zhong and Omary (2004) found that Balb/c and FVB/N mice manifested different susceptibility to injury in two pancreatitis models, induced by cerulein or choline/methionine-deficient, ethionine-supplemented (CDE) diet¹⁴. The same group published a follow-up study in 2017 in which the differential sensitivity was maintained only in the cerulein-induced model²⁰. Proteomic analysis failed to reveal the underlying cause for the difference. Using the experimental models of cerulein administration and CDE diet, Wang et al. (2010) compared 5 mouse strains used in Japan (JF1, C57BL/6J, BALB/c, CBA/J and C3H/HeJ) and documented strain-specific disease outcomes¹⁵. In probably the most detailed study to date, Ulmasov et al. (2013) investigated pancreatitis severity in the J and N substrains of C57BL/6 mice using a cerulein-induced chronic pancreatitis model¹⁶. The authors described stronger pathological responses in C57BL/6J mice relative to the N substrain, however, despite comprehensive gene expression analyses, they were unable to pinpoint

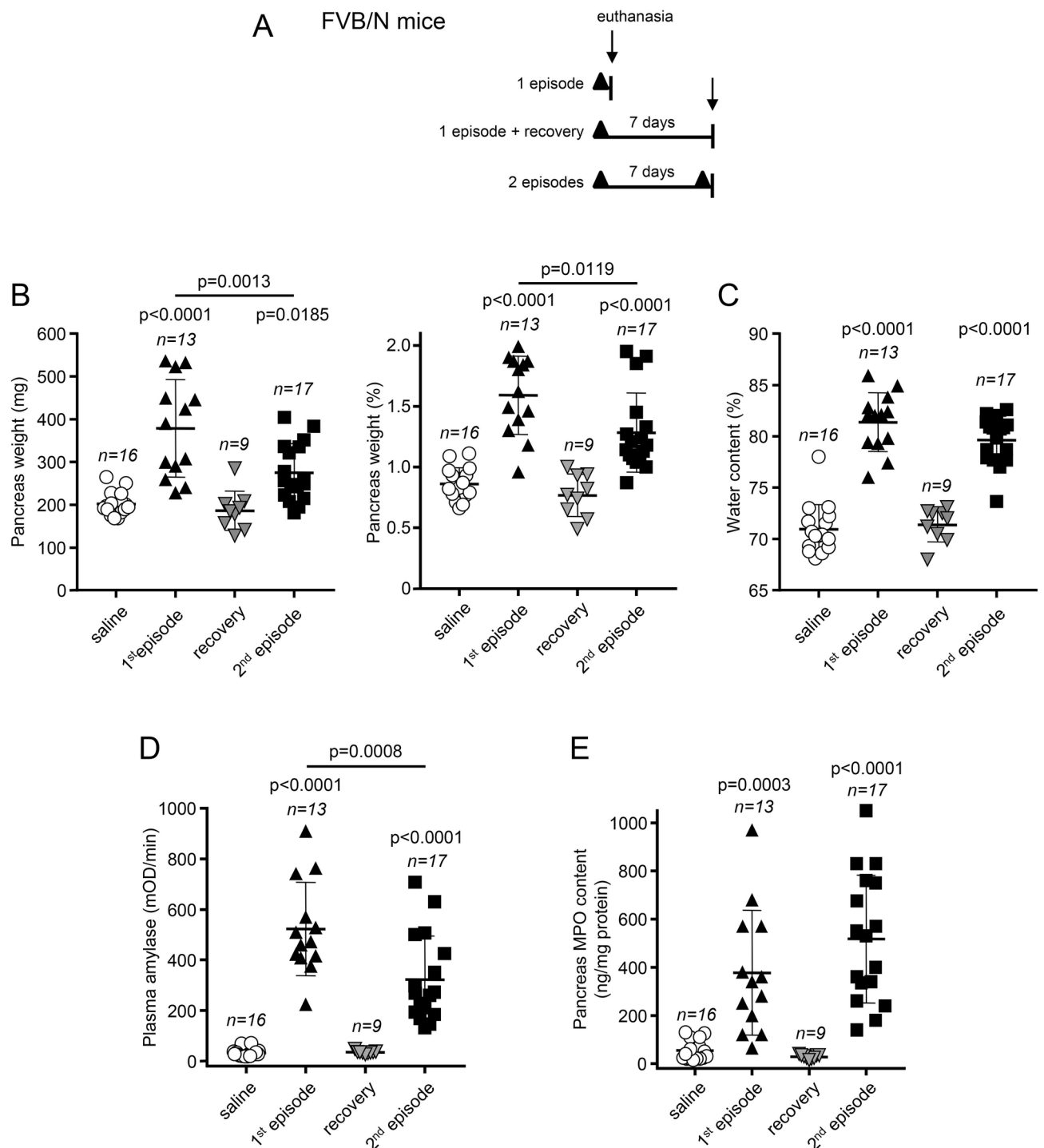


Fig. 6. Cerulein-induced recurrent acute pancreatitis in FVB/N mice. **(A)** Experimental protocol. Solid triangles indicate the two episodes of acute pancreatitis elicited by 10 hourly injections of cerulein on day 1 and day 8. Arrows indicate the time of euthanasia. **(B)** Pancreas weight in mg units and expressed as percent of body weight, **(C)** pancreatic water content, **(D)** plasma amylase activity, and **(E)** pancreatic myeloperoxidase (MPO). For clarity, data from the saline-treated control groups of mice were pooled and graphed as a single group. Individual values with the mean and standard deviation are shown. The difference of means between groups was analyzed by one-way ANOVA and Tukey's post-hoc test.

the genetic cause of this difference. While studying the pain-relieving effect of metamizole during cerulein-induced acute pancreatitis, Stumpf et al. (2016) described that FVB/N mice exhibited more severe disease than C57BL/6J mice¹⁷. Seifert et al. (2017) used ductal taurocholate injection to elicit necrotizing acute pancreatitis in 9 mouse strains and noted diverse pathological responses¹⁸. Finally, in the most recent paper directly relevant

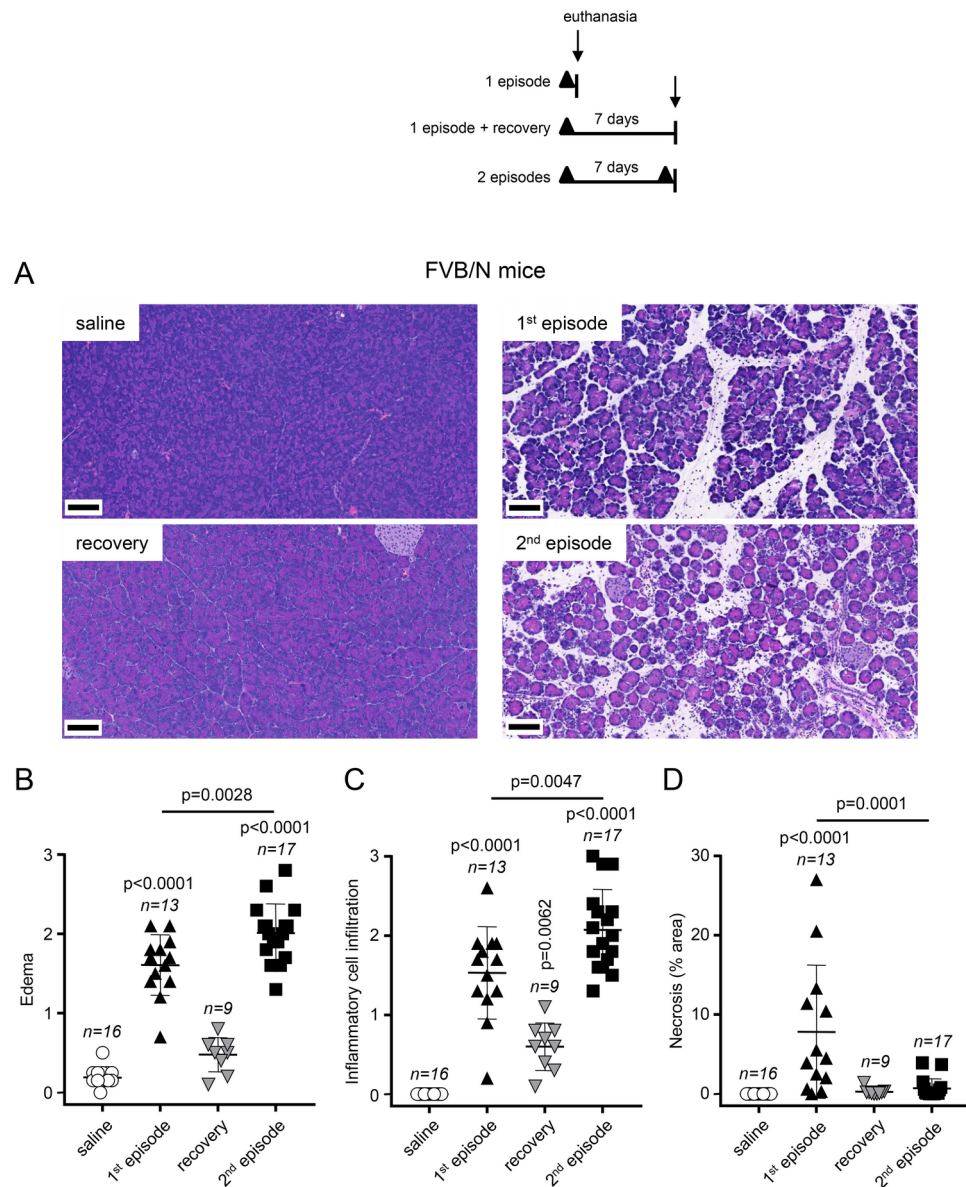


Fig. 7. Histology of cerulein-induced recurrent acute pancreatitis in FVB/N mice. **(A)** Representative hematoxylin–eosin-stained pancreas sections. Scale bars correspond to 100 μm. Histology scoring of pancreas sections for **(B)** edema, **(C)** inflammatory cells, and **(D)** necrosis. For clarity, data from the saline-treated control groups of mice were pooled and graphed as a single group. Individual values with the mean and standard deviation are shown. The difference of means between groups was analyzed by one-way ANOVA and Tukey's post-hoc test.

to our study, Zhang et al. (2017) compared the severity of cerulein-induced acute pancreatitis in FVB/N and C57BL/6 mice, and found that FVB/N mice developed more inflammation and showed delayed regeneration¹⁹. Unfortunately, the authors did not disclose the substrain of the C57BL/6 mice used.

In the present study, we re-visited this problem and compared pathological responses in the C57BL/6N and FVB/N strains in cerulein-induced acute and recurrent acute pancreatitis. Since 2018 we have used C57BL/6N mice to generate various mutant and gene-deleted strains to model hereditary and other forms of genetically-determined pancreatitis^{21–29}. More recently, we used C57BL/6N mice to demonstrate that after a sentinel acute episode, subsequent episodes were more severe¹² and that intrapancreatic trypsin activity is a marker rather than a driver of the early pancreatitis responses¹³. It has remained unclear, however, whether these important observations would hold true in other inbred mouse strains. Therefore, using our routine experimental protocols of cerulein-induced acute pancreatitis, we compared disease severity and intrapancreatic protease activity in C57BL/6N and FVB/N mice.

When a single episode of acute pancreatitis was induced by 10 hourly injections of cerulein, our findings confirmed and extended the published observations, and demonstrated the heightened susceptibility of the FVB/N strain to pancreatic inflammation. To investigate the underlying cause for this phenomenon, we

compared cerulein-induced intrapancreatic trypsin and chymotrypsin activities in pancreas homogenates from the two strains. After a single cerulein injection, we measured not only the early protease activities but also their decline over time. We found higher initial trypsin activity in FVB/N mice which decreased more slowly than in the C57BL/6N strain. While early chymotrypsin peaks were comparable, a slower decay was evident again in FVB/N animals. The reason for the difference in the intrapancreatic trypsin activity can be explained by the lower expression of the trypsin inhibitor SPINK1 and the trypsinogen-degrading lysosomal enzyme CTSL in FVB/N mice relative to C57BL/6N animals. Our recently published data indicated that the early trypsin peak during cerulein-induced intrapancreatic activation does not mediate pathological responses¹³. Therefore, we speculate, the sustained trypsin levels in FVB/N mice may be responsible for the increased severity of pancreatitis. Taken together, we propose that cerulein treatment generates higher intrapancreatic trypsin activity in FVB/N mice, which, in turn, results in stronger pancreatitis responses relative to C57BL/6N mice.

We also investigated whether an episode of cerulein-induced acute pancreatitis would change the severity of a subsequent attack in FVB/N mice. We recently published similar studies with the C57BL/6N strain, where we found that the second pancreatitis episode was more severe than the first, sentinel attack¹². Unexpectedly, here we found that FVB/N mice showed less pancreas edema, lower plasma amylase elevation, and reduced acinar cell necrosis during the second pancreatitis attack when compared to the sentinel episode. We speculate that these seemingly lesser pathological responses during the second pancreatitis episode may be related to the significant acinar cell necrosis observed during the first episode and the incomplete recovery after this attack. In case of the previously studied C57BL/6N mice, acinar cell necrosis was minimal and histological recovery was nearly complete¹². Other parameters, however, indicated increased severity during the second pancreatitis episode in FVB/N mice. Thus, we observed higher MPO levels in pancreas homogenates and increased number of inflammatory cells on histological sections during the second attack; signs of a stronger inflammatory response. Furthermore, there was visibly more histological edema on pancreas sections during the second versus the first pancreatitis episode. Hegyi et al. (2021) reported similar results of lower serum amylase and higher inflammatory cells during the second versus the first episodes of cerulein-induced pancreatitis in FVB/N mice³⁰. Similarly to our protocol, the authors used 10 hourly injections of cerulein to induce the acute attacks but allowed only 3 days for recovery, suggesting that the second attack might have been elicited in a partly inflamed pancreas. Del Poggetto et al. (2021) also published similar findings with C57BL/6J mice, where lower serum amylase levels were detected during the second attack after a 4-week recovery period³¹. Taken the published and new data together, it appears that pathological responses during recurrent attacks in mice strongly depend on the mouse strain and the experimental protocol employed. The severity of the sentinel episode, acinar cell necrosis in particular, and the recovery time before the second episode are likely the strongest determinants of severity in the second episode.

In summary, using C57BL/6N and FVB/N mice, we confirmed and extended prior observations that inbred mouse strains exhibit differences in their pathological responses during acute and recurrent acute pancreatitis. The results argue that considering the genetic background is critical for the correct interpretation of experimental pancreatitis data. Limitations of our study include the lack of a detailed analysis of the inflammatory microenvironment and associated intracellular signaling pathways that would provide further mechanistic insights. It is possible that besides cathepsin L and SPINK1 levels, differences in other factors such as calcium signaling in acinar cells and/or immune cells affect trypsinogen activation in a strain-dependent manner. As highlighted in a review by Petersen et al. (2021)³², aberrant intracellular calcium signaling through various calcium channels can drive pathological acinar cell responses, including premature zymogen activation, ATP depletion, and cell death. Additionally, sustained calcium influx into stellate cells and macrophages may exacerbate these pathogenic responses^{33–35}. A detailed examination of these cellular interactions would provide a deeper and more comprehensive understanding of strain-dependent susceptibility to experimental pancreatitis.

Methods

Animals

C57BL/6N and FVB/N mice were obtained from Charles River Laboratories (Wilmington, MA) or produced in our breeding facilities from the same stock. Both male and female mice were studied. The number of mice used in the experiments are shown in the figures.

Study approval

Animal studies were conducted in agreement with the animal research: reporting of in vivo experiments (ARRIVE) guidelines. Experiments were performed at the University of California Los Angeles with the approval and oversight of the Animal Research Committee, including protocol review and post-approval monitoring and at Boston University with the approval and oversight of the Institutional Animal Care and Use Committee (IACUC). The animal care programs at these institutions are managed in full compliance with the US Animal Welfare Act, the United States Department of Agriculture Animal Welfare Regulations, the US Public Health Service Policy on Humane Care and Use of Laboratory Animals and the National Research Council's Guide for the Care and Use of Laboratory Animals. The University of California Los Angeles and Boston University have approved Animal Welfare Assurance statements on file with the US Public Health Service, National Institutes of Health, Office of Laboratory Animal Welfare. Both institutions are accredited by the Association for Assessment and Accreditation of Laboratory Animal Care International (AAALAC). All experiments were approved by the Boston University Institutional Biosafety Committee (IBC). All methods were performed in accordance with the relevant guidelines and regulations, including those established by the IBC and applicable institutional and national biosafety standards.

Cerulein-induced acute pancreatitis

Acute pancreatitis was induced in 9–10-week-old mice with 10 intraperitoneal injections of the secretagogue peptide cerulein (50 µg/kg dose, catalog number C9026, Sigma-Aldrich, St. Louis, Missouri), administered hourly. Control animals received saline injections. To assess severity of a single acute pancreatitis attack, mice were euthanized 1 h after the last injection. To evaluate the degree of recovery after an episode of acute pancreatitis, mice were euthanized 7 days after the last cerulein injection. Mice undergoing two episodes of pancreatitis were euthanized 1 h after the second series of cerulein injections. Euthanasia was performed using CO₂ asphyxiation, followed by cervical dislocation. Pancreas tissue and blood were harvested.

Pancreatic water content

Approximately 50 mg pancreatic tissue was weighed (wet weight), dried for 72 h at 65 °C, and weighed again (dry weight). Tissue water content was calculated by subtracting the dry weight from the wet weight value and then expressed as percent of the wet weight.

Plasma amylase activity and tissue amylase content

For plasma amylase activity, blood was collected through cardiac puncture with heparinized syringes, and plasma was isolated by centrifuging blood samples at 2000g for 15 min at 4 °C. Amylase activity was determined from 1 µL of plasma diluted with 9 µL normal saline and mixed with 190 µL of 2-chloro-*p*-nitrophenyl- α -D-maltotriose substrate (catalog number A7564-60, Pointe Scientific, Canton, MI). The increase in absorbance due to the release of 2-chloro-nitrophenol was monitored in a microplate reader at 405 nm for 2 min. Rate of substrate cleavage was expressed in mOD/min units.

Tissue amylase content was determined from pancreas homogenates. Briefly, 30–40 mg pancreas tissue was homogenized in 300–400 µL ice-cold 20 mM Na-HEPES (pH 7.4) buffer. To remove heavy particulate matter, homogenates were centrifuged at 850g for 10 min at 4 °C. Amylase activity was measured from 1 µL of 100× diluted homogenate, as described above. The rate of substrate cleavage was normalized to the total protein content and expressed as percent of a designated reference value, as indicated in the figure legends.

Pancreatic myeloperoxidase content

Myeloperoxidase (MPO) content was determined using an ELISA kit (catalog number HK210-01, Hycult Biotech, Plymouth Meeting, PA) according to the manufacturer's instructions, as described previously³⁶. The absorbance measured at 450 nm was converted to ng/mL MPO concentration using a calibration curve, normalized to total protein concentration, and expressed in ng MPO/mg protein units.

Intrapancreatic trypsin and chymotrypsin activity

Cerulein-induced intrapancreatic protease activity was determined at 30 min, 2, 4 and 8 h after a single cerulein injection (50 µg/kg body weight dose), as described previously³⁷. The rate of substrate cleavage was normalized to the total protein in the assay mixture and enzyme activity was expressed as relative fluorescent units (RFU) per sec per mg protein.

Histology

Pancreas tissue was fixed in 10% neutral buffered formalin, paraffin-embedded, sectioned, and stained with hematoxylin–eosin at the Translational Pathology Core Laboratory of University of California Los Angeles and at the Boston University Experimental Pathology Laboratory Service Core. Histology slides were digitalized using the Panoramic DESK slide scanner and evaluated for edema, inflammatory cell infiltration, and necrosis as described previously³⁸.

Pancreatic protease zymogen content

To determine the total pancreatic trypsinogen, chymotrypsinogen and proelastase content of C57BL/6N and FVB/N mice (10 weeks of age), 30–40 mg pancreas tissue was homogenized in 300–400 µL ice-cold 20 mM Na-HEPES (pH 7.4) buffer and centrifuged at 850g for 10 min at 4 °C. To activate protease zymogens, 5 µL aliquot of the supernatant was treated with 50× diluted human enteropeptidase (catalog number 1585-SE, R&D Systems; 4 µL was used for trypsinogen activation and 2 µL for chymotrypsinogen and proelastase activation) in 100 µL final volume of 0.1 M Tris–HCl (pH 8.0), 10 mM CaCl₂ and 0.05% Tween-20. Enzyme activities were followed every 5 min by withdrawing a 2 µL aliquot and mixing it with 48 µL assay buffer (0.1 M Tris–HCl at pH 8.0, 1 mM CaCl₂, 0.05% Tween-20) and 150 µL 200 µM substrate dissolved in assay buffer (N-CBZ-Gly-Pro-Arg-pNA for trypsin, Suc-Ala-Ala-Pro-Phe-pNA for chymotrypsin, and Suc-Ala-Ala-Pro-Ala-pNA for elastase). The increase in absorbance was monitored in a microplate reader at 405 nm. The rate of substrate cleavage was normalized to the total protein content of the reaction and results were expressed as percent of the average of C57BL/6N values.

Protein measurement

To determine the total pancreatic protein content in C57BL/6N and FVB/N mice, we used pancreas homogenates as described above. The homogenate was diluted ten-fold and 2 µL was mixed with 8 µL water and 190 µL of the colorimetric Pierce™ Bradford Plus Protein Assay Reagent (Thermo Scientific, catalog number 23238). The absorbance was measured in a microplate reader at 595 nm and converted to mg units using a calibration curve prepared with bovine serum albumin. Results was expressed as mg protein per mg tissue.

DNA measurement

To determine the total DNA content in pancreas homogenates from C57BL/6N and FVB/N mice, we used a slightly modified version of a published protocol³⁹. Briefly, 30–40 mg pancreas tissue was homogenized in 300–400 μ L 20 mM Na-HEPES (pH 7.4) buffer and sonicated for 20 s. The homogenate (4 μ L) was mixed with 2 μ L 0.1 mg/mL Hoechst 33,258 stain (Thermo Fisher, H3569, 10 mg/mL stock solution diluted 100 \times in water) and 194 μ L 20 mM Na-HEPES buffer. The fluorescence was measured in a plate reader at 356 nm excitation and 458 nm emission wavelengths. Fluorescence units were converted to DNA concentration using a calibration curve prepared with calf thymus DNA (Thermo Fisher, 15,633–019, diluted in 20 mM Na-HEPES buffer). Results were expressed as μ g DNA per mg tissue.

Western blot and densitometry

For western blotting, 30–40 mg pancreas tissue from 10-week-old mice was homogenized in 300–400 μ L ice-cold PBS (pH 7.4) supplemented with Halt protease and phosphatase inhibitor (catalog number 78440, Thermo Scientific) and centrifuged at 13,500 rpm for 10 min at 4 °C. 30 μ g homogenate was electrophoresed SDS-PAGE minigels, and transferred onto an Immobilon-P membrane (catalog number IPVH00010, MilliporeSigma). After blocking with 10% solubilized milk powder, the membrane was incubated with the primary antibody overnight at 4 °C and then with the secondary antibody for 1 h at room temperature. Cationic (T7) trypsinogen and ERK1/2 were detected using SuperSignal West Pico chemiluminescent substrate (catalog number 34580, Thermo Scientific). SPINK1 protein was detected by SuperSignal West Femto Maximum Sensitivity chemiluminescent substrate (catalog number 34095, Thermo Scientific). ERK1/2 loading control was detected on the same membranes following stripping. Antibodies and dilutions were as follows. Cationic (T7) trypsinogen was detected using a custom-made rabbit polyclonal antibody at a 1:10,000 dilution²¹. A rabbit polyclonal antibody against mouse SPINK1 was used at a dilution of 1:1,000 (catalog number 2744, Cell Signaling Technology, Danvers, MA). A rabbit monoclonal antibody against ERK1/2 (p44/42 MAPK 137F5) was used at 1:1,000 dilution (catalog number 4695, Cell Signaling Technology, Danvers, MA). A rabbit monoclonal antibody against CTSE was used at 1:1,000 dilution (catalog number ab214428, Abcam). A polyclonal goat antibody against CTSL was used at 1:1,000 dilution (catalog number AF1515, R&D Systems). A horseradish peroxidase (HRP)-conjugated goat anti-rabbit IgG (catalog number HAF008, R&D Systems) was used at 1:10,000 dilution to detect (T7) trypsinogen, SPINK1, and ERK1/2, and at 1:5000 dilution to detect CTSE. A HRP-conjugated anti-goat IgG (catalog number HAF109, R&D Systems) was used at 1:5000 dilution to detect CTSL. Densitometric evaluation was performed using the ImageJ software (version 1.52a).

Statistical analyses

Experimental results were graphed as individual data points with the mean and standard deviation (SD) indicated. Difference of means was analyzed by unpaired *t*-test when comparing two groups, and by one-way ANOVA followed by Tukey's post-hoc analysis in case of multiple groups (GraphPad Prism). Statistical significance was defined as $p < 0.05$, and p values were shown in the figures when the difference was significant.

Data availability

Materials, datasets, and protocols associated with the study are available from the corresponding author upon request.

Received: 2 October 2024; Accepted: 15 April 2025

Published online: 08 May 2025

References

- Yadav, D. & Lowenfels, A. B. The epidemiology of pancreatitis and pancreatic cancer. *Gastroenterology* **144**, 1252–1261 (2013).
- Yadav, D., O'Connell, M. & Papachristou, G. I. Natural history following the first attack of acute pancreatitis. *Am. J. Gastroenterol.* **107**, 1096–1103 (2012).
- Sankaran, S. J. et al. Frequency of progression from acute to chronic pancreatitis and risk factors: A meta-analysis. *Gastroenterology* **149**, 1490–1500 (2015).
- Mayerle, J. et al. Genetics, cell biology, and pathophysiology of pancreatitis. *Gastroenterology* **156**, 1951–1968 (2019).
- Sahin-Tóth, M. & Hegyi, P. Smoking and drinking synergize in pancreatitis: Multiple hits on multiple targets. *Gastroenterology* **153**, 1479–1481 (2017).
- Lerch, M. M. & Gorelick, F. S. Models of acute and chronic pancreatitis. *Gastroenterology* **144**, 1180–1193 (2013).
- Gorelick, F. S. & Lerch, M. M. Do animal models of acute pancreatitis reproduce human disease?. *Cell. Mol. Gastroenterol. Hepatol.* **4**, 251–262 (2017).
- Saloman, J. L. et al. Animal models: Challenges and opportunities to determine optimal experimental models of pancreatitis and pancreatic cancer. *Pancreas* **48**, 759–779 (2019).
- Bartholomew, C. Acute scorpion pancreatitis in Trinidad. *BMJ* **5697**, 666–668 (1970).
- Marsh, W. H., Vukov, G. A. & Conradi, E. C. Acute pancreatitis after cutaneous exposure to an organophosphate insecticide. *Am. J. Gastroenterol.* **83**, 1158–1160 (1988).
- Mayerle, J., Sandler, M. & Lerch, M. M. Secretagogue (Caerulein) induced pancreatitis in rodents. *Pancreapedia Exocrine Pancreas Knowl. Base* (2013). <https://doi.org/10.3998/panc.2013.2>
- Geisz, A. & Sahin-Tóth, M. Sentinel acute pancreatitis event increases severity of subsequent episodes in mice. *Gastroenterology* **161**, 1692–1694 (2021).
- Geisz, A., Tran, T., Orekhova, A. & Sahin-Tóth, M. Trypsin activity in secretagogue-induced murine pancreatitis is solely elicited by cathepsin B and does not mediate key pathologic responses. *Gastroenterology* **164**, 684–687 (2023).
- Zhong, B. & Omary, M. B. Actin overexpression parallels severity of pancreatic injury. *Exp. Cell Res.* **299**, 404–414 (2004).
- Wang, J. et al. Relationship of strain-dependent susceptibility to experimentally induced acute pancreatitis with regulation of *Prss1* and *Spink3* expression. *Lab. Invest.* **90**, 654–664 (2010).

16. Ulmasov, B., Oshima, K., Rodriguez, M. G., Cox, R. D. & Neuschwander-Tetri, B. A. Differences in the degree of cerulein-induced chronic pancreatitis in C57BL/6 mouse substrains lead to new insights in identification of potential risk factors in the development of chronic pancreatitis. *Am. J. Pathol.* **183**, 692–708 (2013).
17. Stumpf, F. et al. Metamizol relieves pain without interfering with cerulein-induced acute pancreatitis in mice. *Pancreas* **45**, 572–578 (2016).
18. Seifert, G. J., Sander, K. C., Richter, S. & Wittel, U. A. Murine genotype impacts pancreatitis severity and systemic inflammation: An experimental study. *Ann. Med. Surg. (Lond.)* **24**, 8–14 (2017).
19. Zhang, X., Shi, Q., Wang, C. & Wang, G. Differential susceptibility of mouse strains on pancreatic injury and regeneration in cerulein-induced pancreatitis. *Int. J. Clin. Exp. Pathol.* **10**, 9934–9944 (2017).
20. Iyer, S. et al. Clusterin and Pycr1 alterations associate with strain and model differences in susceptibility to experimental pancreatitis. *Biochem. Biophys. Res. Commun.* **482**, 1346–1352 (2017).
21. Geisz, A. & Sahin-Tóth, M. A preclinical model of chronic pancreatitis driven by trypsinogen autoactivation. *Nat. Commun.* **9**, 5033 (2018).
22. Jancsó, Z., Hegyi, E. & Sahin-Tóth, M. Chymotrypsin reduces the severity of secretagogue-induced pancreatitis in mice. *Gastroenterology* **155**, 1017–1021 (2018).
23. Jancsó, Z. & Sahin-Tóth, M. Mutation that promotes activation of trypsinogen increases severity of secretagogue-induced pancreatitis in mice. *Gastroenterology* **158**, 1083–1094 (2020).
24. Mosztbacher, D., Jancsó, Z. & Sahin-Tóth, M. Loss of chymotrypsin-like protease (CTRL) alters intrapancreatic protease activation but not pancreatitis severity in mice. *Sci. Rep.* **10**, 11731 (2020).
25. Orekhova, A. et al. Evolutionary expansion of polyaspartate motif in the activation peptide of mouse cationic trypsinogen limits autoactivation and protects against pancreatitis. *Am. J. Physiol. Gastrointest. Liver Physiol.* **321**, G719–G734 (2021).
26. Mosztbacher, D. & Sahin-Tóth, M. Mouse model suggests limited role for human mesotrypsin in pancreatitis. *Pancreatol.* **21**, 342–352 (2021).
27. Demcsák, A. & Sahin-Tóth, M. Rate of autoactivation determines pancreatitis phenotype in trypsinogen mutant mice. *Gastroenterology* **163**, 761–763 (2022).
28. Jancsó, Z., Morales Granda, N. C., Demcsák, A. & Sahin-Tóth, M. Mouse model of PRSS1 pR122H-related hereditary pancreatitis highlights context-dependent effect of autolysis-site mutation. *Pancreatol.* **23**, 131–142 (2023).
29. Demcsák, A., Shariatzadeh, S. & Sahin-Tóth, M. Secretagogue-induced pancreatitis in mice devoid of chymotrypsin. *Am. J. Physiol. Gastrointest. Liver Physiol.* **327**, G333–G344 (2024).
30. Hegyi, P. J. et al. Evidence for diagnosis of early chronic pancreatitis after three episodes of acute pancreatitis: A cross-sectional multicentre international study with experimental animal model. *Sci. Rep.* **11**, 1367 (2021).
31. Del Poggetto, E. et al. Epithelial memory of inflammation limits tissue damage while promoting pancreatic tumorigenesis. *Science* **373**, eabj0486 (2021).
32. Petersen, O. H., Gerasimenko, J. V., Gerasimenko, O. V., Gryshchenko, O. & Peng, S. The roles of calcium and ATP in the physiology and pathology of the exocrine pancreas. *Physiol. Rev.* **101**, 1691–1744 (2021).
33. Gryshchenko, O., Gerasimenko, J. V., Gerasimenko, O. V. & Petersen, O. H. Ca(2+) signals mediated by bradykinin type 2 receptors in normal pancreatic stellate cells can be inhibited by specific Ca(2+) channel blockade. *J. Physiol.* **594**, 281–293 (2016).
34. Gryshchenko, O., Gerasimenko, J. V., Petersen, O. H. & Gerasimenko, O. V. Calcium signaling in pancreatic immune cells in situ. *Function (Oxford, England)* **2**, zqaa026 (2020).
35. Vigna, S. R. & Liddle, R. A. Calcium in pancreatitis ... Immune cells, too?. *Function (Oxford, England)* **2**, zqaa030 (2021).
36. Hegyi, E. & Sahin-Tóth, M. Human CPA1 mutation causes digestive enzyme misfolding and chronic pancreatitis in mice. *Gut* **68**, 301–312 (2019).
37. Mosztbacher, D., Demcsák, A. & Sahin-Tóth, M. Measuring digestive protease activation in the mouse pancreas. *Pancreatol.* **20**, 288–292 (2020).
38. Demcsák, A. & Sahin-Tóth, M. Heterozygous *Spink1* deficiency promotes trypsin-dependent chronic pancreatitis in mice. *Cell Mol. Gastroenterol. Hepatol.* **18**, 101361 (2024).
39. Labarca, C. & Paigen, K. A simple, rapid, and sensitive DNA assay procedure. *Anal. Biochem.* **102**, 344–352 (1980).

Acknowledgements

This work was supported by the National Institutes of Health (NIH) grants R01 DK132471 (to A.G.-F.), R01 DK117809 and R01 DK082412 (to M.S.-T.), the American Pancreatic Association Young Investigator in Pancreatitis grant Agmt dtd 7/1/2020 (to A.G.-F.), the National Pancreas Foundation award 20233127 (to A.D.), and the Department of Defense Grant HT9425-24-1-0164, PR230469 (to A.D.).

Author contributions

A.G.-F. and M.S.-T. conceived and directed the study; A.G.-F., M.S.-T., A.D., and T.T. designed the experiments; A.G.-F., A.D. and T.T. performed the experiments; A.G.-F., M.S.-T., A.D., and T.T. analyzed the data; A.G.-F., A.D., and M.S.-T. wrote the manuscript; A.G.-F. and A.D. prepared the figures. All authors contributed significant revisions to the manuscript and approved the final version.

Declarations

Competing interests

The authors declare no competing interests.

Additional information

Supplementary Information The online version contains supplementary material available at <https://doi.org/10.1038/s41598-025-98914-z>.

Correspondence and requests for materials should be addressed to A.G.-F.

Reprints and permissions information is available at www.nature.com/reprints.

Publisher's note Springer Nature remains neutral with regard to jurisdictional claims in published maps and institutional affiliations.

Open Access This article is licensed under a Creative Commons Attribution-NonCommercial-NoDerivatives 4.0 International License, which permits any non-commercial use, sharing, distribution and reproduction in any medium or format, as long as you give appropriate credit to the original author(s) and the source, provide a link to the Creative Commons licence, and indicate if you modified the licensed material. You do not have permission under this licence to share adapted material derived from this article or parts of it. The images or other third party material in this article are included in the article's Creative Commons licence, unless indicated otherwise in a credit line to the material. If material is not included in the article's Creative Commons licence and your intended use is not permitted by statutory regulation or exceeds the permitted use, you will need to obtain permission directly from the copyright holder. To view a copy of this licence, visit <http://creativecommons.org/licenses/by-nc-nd/4.0/>.

© The Author(s) 2025